JOINT EUROPEAN TORUS JET

JET–P(93)22

N.P. Hawkes, P. van Belle, P. Dixon, M.A. Hone,
O.N. Jarvis, M.J. Loughlin, M.T. Swinhoe

A 2.5MeV Neutron Spectrometry System with a Tangential Line of Sight for the D-D Phase at the JET Tokamak*

A 2.5MeV Neutron Spectrometry System with a Tangential Line of Sight for the D-D Phase at the JET Tokamak*

N.P. Hawkes[1], P. van Belle, P. Dixon[1], M.A. Hone,
O.N. Jarvis, M.J. Loughlin, M.T. Swinhoe[2]

JET-Joint Undertaking, Culham Science Centre, OX14 3DB, Abingdon, UK

[1]AEA Industrial Technology, Harwell Laboratory, Didcot, Oxon, OXll ORA, UK.
[2]AEA Industrial Technology, Harwell Laboratory, Didcot, Oxon, OXll ORA, UK.
Present address: CEC, Directorate of Euratom Safeguards, Cube Building, Luxembourg.

** This work was funded by JET under contracts JBl/9001, JE2/0685 and JE6/0163.*
Additional support was provided by the UK Fusion Programme under a Task Agreement.
The spectrometry system was designed, constructed, installed and commissioned by AEA Technology.

Preprint of a paper to be submitted for publication in N.I.M
April 1993

ABSTRACT

The neutron spectrometry system described in this report is in routine use at the Joint European Torus (JET). Designed for the D-D phase of operations, it consists of a complementary set of compact neutron spectrometers housed in a shielding block in the Torus Hall.

The block is raised by a tower to the level of the mid plane of the torus. The collimation system, which has an adjustable aperture, defines a horizontal line of sight with a significant directional component tangential to the plasma axis.

The shielding, the spectrometers, and the auxiliary sensors and systems are described. The operating limits of the spectrometers, and the methods of data analysis, are discussed. Examples of analysed data are given.

1. INTRODUCTION

1.1 Neutron Spectrometry at JET

One of the most promising approaches to power production by controlled nuclear fusion is the magnetic confinement of hot plasmas in large tokamaks (plasma devices with toroidal geometry). The Joint European Torus (JET) is one such device, designed to study plasma behaviour in conditions close to those in a future fusion reactor [1].

The velocity distributions of the ions in the plasma are an important aspect of plasma behaviour. Neutron spectrometry provides uniquely direct information on these distributions (as described in later sections), and is in routine use at JET [2]. Two diagnostic systems have been installed for this purpose: one is in the Roof Laboratory above the JET machine, and views the plasma along a vertical line of sight [3]; the other is in the Torus Hall itself, and views the plasma horizontally. It is the latter system which is described here. Examples of the information it provides are given, and the advantages of its line of sight are discussed.

1.2 Plasma Heating

The way in which the plasma is heated has a profound effect on the velocity distribution of the ions in it. In a tokamak, the basic heating mechanism is the ohmic heating produced by the large current which flows through the plasma. This current is induced by transformer action, so the period over which it can be sustained is limited by the volt seconds available from the transformer. Tokamaks are therefore inherently pulsed devices. In JET, a pulse lasts about 20 seconds, with about 10 seconds of steady plasma current at 3 - 5 MA typically. The ion velocity distribution produced by ohmic heating is thermal (Maxwellian), and in JET the average kinetic energy in a typical ohmic plasma is a few keV.

Additional heating is often employed in plasma experiments to raise the temperature of the plasma beyond that attainable by ohmic heating alone. At JET, two types of additional heating are avialable: Ion Cyclotron Resonance Heating (ICRH), and Neutral Beam Injection (NBI).

In ICRH, electromagnetic radiation at radio frequencies is launched into the plasma from antennas inside the vacuum vessel. The frequency is chosen to match the cyclotron resonance of some minority ion species in the plasma, such as ^{3}He. Up to 22 MW can be introduced in this way [4]. In NBI, beams of neutral hydrogen, deuterium or helium are directed into the plasma from injector units outside the magnetic confinement. The injectors at JET provide neutral beams at energies from 80 to 140 keV, delivering up to about 19 MW total power [4]. Both ICRH and NBI produce a significant population of ions with a non-Maxwellian velocity distribution.

1.3 Neutron Production in Tokamak Plasmas

Fusion between the hydrogen isotopes deuterium and tritium is currently thought the most likely reaction to be used in a future fusion reactor. However, the copious high energy neutrons associated with it pose serious problems of activation and shielding. Most tokamak experiments to date have therefore used deuterium (D-D) plasmas rather than deuterium/ tritium (D-T) plasmas.

The spectrometry system described here is intended for use with deuterium plasmas, ie during the 'D-D phase' of JET operations prior to the routine use of tritium.

Deuterium plasmas produce predominantly 2.5 MeV neutrons, with a much smaller flux at 14 MeV. The neutron production mechanisms are discussed briefly below.

1.3.1 2.5 MeV Neutrons

The two principal fusion reactions in a deuterium plasma are

$$D + D \rightarrow {}^{3}He + n,\ Q = 3.27\ \text{MeV} \qquad (1)$$

and

$$D + D \rightarrow T + p,\ Q = 4.03\ \text{MeV} \qquad (2)$$

with roughly equal probability. The neutron produced in reaction (1), being uncharged, escapes readily from the plasma, carrying with it important information on plasma conditions. For example:

1) The rate of production of neutrons provides a direct measure of the rate of fusion.

2) The energy spectrum of the neutrons carries information on the velocity distribution of the duetrons (because the spectrum, which would be a single line at E_n = 2.45 MeV in a cold plasma, is Doppler broadened in a hot plasma by the motion of the deuterons).

It is the second of these effects which is the basis of neutron spectrometry as a plasma diagnostic. The information obtainable from neutron spectrometry is discussed briefly in Section 1.4, and more detailed examples are given in the section on Analysis.

1.3.2 *14 MeV Neutrons*

The triton produced in reaction (2) can undergo a secondary fusion reaction with a deuteron to produce a 14 MeV neutron:

$$T + D -> \alpha + n, \; Q = 17.6 \text{ MeV} \qquad (3)$$

At JET, this results in a flux of 14 MeV neutrons with an intensity about 1% that of the 2.5 MeV flux. The spectrometry system described here is not intended to perform measurements on 14 MeV neutrons, but their effect as a source of background had to be considered during the design.

1.4 Neutron Spectrometry in Plasma Diagnostics

In a deuterium plasma heated purely ohmically, the deuteron velocity distribution is thermal (Maxwellian). This produces a Gaussian neutron energy spectrum with a full width at half maximum (FWHM) of $82.5\sqrt{T_i}$ keV approximately, where T_i is the ion temperature in keV [5, 6]. Hence the ion temperature of an ohmic plasma can be determined directly from neutron spectrometry.

The presence of non-Gaussian components in the neutron spectrum indicates non-thermal ion populations in the plasma, or even the presence of neutron production mechanisms other than the fusion of deuterons. For example, neutrons can be produced by reactions between thermal deuterons and fast deuterons injected by the Neutral Beam Injectors; or ions can be accelerated by high power Radio Frequency heating, and produce neutrons by reactions with beryllium or carbon impurities.

Such neutrons can have energies in the range 2 to 8 MeV. The examples given in the Analysis section below show how neutron spectrometry can measure the relative strengths of several thermonuclear and non-thermonuclear neutron production mechanisms, which is essential information for the interpretation of neutron yield measurements.

Other areas in which neutron spectrometry has an important role include the determination of the central deuteron to electron density ratio, as discussed by Jarvis et al. [7].

1.5 The JET 2.5 MeV Spectrometry System with Tangential Line of Sight

The system described here consists of a complementary set of neutron spectrometers, contained in the 1.1 m^3 internal cavity of a large hollow shielding block inside the JET Torus Hall. A tower raises the block to the level of the mid-plane of the torus, giving the spectrometers a collimated horizontal line of sight which has a significant directional component tangential to the axis of the plasma. This line of sight allows the observation of certain phenomena which are not apparent when the plasma is viewed from above, i.e. radially to the axis of the plasma. (One example of this, described in greater detail in Section 6.1.3, is the effect of injected deuterons in trapped orbits). The line of sight passes through an adjustable aperture just outside the JET vacuum vessel. This extends the range of neutron yields over which the spectrometers can operate by roughly an order of magnitude. The shield and the line of sight are described in more detail in Section 2 below.

As no single spectrometer could meet all the requirements of the JET system, a set of complementary devices is installed. Four spectrometers are available for use, of which three are usually present together; a summary of their characteristics appears in Table 1, and a detailed description is given in Section 3.

TABLE 1:
Summary of the available spectrometers and their characteristics.
(For further details see Section 3).

Description	Approximate Resolution, keV FWHM at 2.5 MeV	Efficiency, Counts Per (n / cm^2)	JET Yield Range,* n / s	Comments
^{3}He Gridded Ionisation Chamber	70 (effective)	1.0×10^{-2} (counts in fast peak)	1.0×10^{14} to 5.0×10^{15}	Excellent resolution, but efficiency low. Limit of $E_n < 3$ MeV imposed by wall effects. Counting rate limited by long charge collection times.
Organic Liquid Scintillator 5 cm dia. x 1 cm thick	215	4.8×10^{-1} (counts above $E_p = 2$ MeV)	1.0×10^{14} to 5.0×10^{15}	Poorer resolution, but efficiency remains high even for high neutron energies. Capable of high counting rates. Spectra hard to analyse fully.
Organic Liquid Scintillator 1 cm dia. x 1 cm thick	215	2.0×10^{-2} (counts above $E_p = 2$ MeV)	above 5.0×10^{15}	As above
Proton Recoil Telescope	230	1.0×10^{-4} (counts in peak)	above 5.0×10^{15}	Poorer resolution than scintillator, but relatively insensitive to gamma rays, and form of response makes analysis easier. Capable of high counting rates.

Locating the spectrometers in the Torus Hall offers the advantages of a tangential line of sight, but does impose constraints on available space and ease of access. Consequently only compact spectrometers with low maintenance requirements can be used. This rules out systems such as the time-of-flight spectrometer installed in the Roof Laboratory [3], which provides high performance but is large and complex.

Various auxiliary systems and sensors maintain and monitor the environment within the shield cavity. For example, a chiller keeps the temperature at about 15°C, and temperature probes verify that this is operating correctly. Other sensors record the magnetic field inside the enclosure, for subsequent checking against

* Approximate range of JET neutron emission rates within which spectrometer gives useful results for an individual pulse. Details depend on duration of additional heating and setting of adjustable aperture.

the allowable limits for the scintillation spectrometers. The auxiliary systems are described more fully in Section 4.

The monitoring of the spectrometers and the acquisition of the data are described in Section 5, and the methods of analysis are discussed in Section 6.

2. THE SHIELDING BLOCK AND ITS LINE OF SIGHT

2.1 The Tower and Shielding Block

The shielding block and its tower are shown in Fig. 1. The tower is 4.86 m high, and made of a stainless steel tube 40 cm in diameter. Location pegs in the floor of the Torus Hall ensure that the tower can always be replaced in precisely the same position.

The shielding block is primarily a neutron shield. (Gamma shielding is described below). The material is principally a mixture of 90% paraffin wax and 10% lithium carbonate. The hydrogenous wax attenuates the fast components of the neutron flux, and the lithium is highly effective against the slow component because of its large (non-radiative) capture cross section. Similar shielding material is described by Glasgow et al. [8]. The block was constructed by pouring a mixture of molten paraffin wax and fine lithium carbonate powder into a hollow stainless steel shell, which now provides the mechanical strength. The internal cavity for the spectrometers measures 60 cm wide by 100 cm high by 180 cm long, and the shielding is 100 cm thick at the front and 60 cm thick elsewhere. The total mass of the block is approximately 13 tonnes. At the back, a section of the shield can be lowered on a pair of motorised screw jacks to provide access to the spectrometers.

There are three small penetrations (25 - 50 mm diameter) in the shielding block for cables and pipes.

Each time the shielding block is replaced on the tower, its alignment is checked using two lasers. These are fixed rigidly to its sides and direct their beams on to targets on the Torus Hall wall and on the JET machine. Reproducibility to better than one milliradian is easily obtained.

2.2 The Line of Sight and Adjustable Aperture

The line of sight is defined by a polythene collimator 2.2 m long with a circular channel 60 mm diameter, and is shown in Fig. 2. It enters the JET vacuum vessel via the Octant 4 port, passes close to (but does not touch) the central column, and terminates in the Octant 7 port (well away from the plasma, to reduce the flux of backscattered neutrons). As mentioned above, there is a significant directional component tangential to the plasma axis. The distance from the spectrometers to the nearest portion of the core of the plasma is about 11 m.

There is an adjustable aperture (not shown in Fig. 1) roughly mid way between the outer end of the collimator and the Octant 4 port window. It consists of two pairs of 30 cm thick steel jaws, one of which defines the horizontal extent of the aperture and the other the vertical. They are set to suit the expected neutron yield, using a remotely controlled servo mechanism implemented via the JET "CODAS" control and data acquisition system [9]. The left hand jaw is set in such a way that the field of view of the spectrometers does not include the central column of the vessel.

2.3 Gamma Ray and Other Shielding

Some shielding against gamma rays is provided by a wall of lead 50 mm thick at the front of the cavity. In addition, the spectrometers are surrounded by lead shielding approximately 60 mm thick (see Fig. 3), constructed mainly from individually tailored lead rings stacked back to back. The total mass of the gamma shielding is approximately one tonne.

A lead disc and a boron disc, both 1 cm thick, are placed inside the polythene collimator to attenuate gamma rays and slow neutrons respectively.

3. THE SPECTROMETERS

3.1 Introduction

The range of neutron energies of interest is large (2 to 8 MeV), and the range of yields to be covered is extremely so (three to four order of magnitude). For this reason, and to provide some redundancy, four different spectrometers

with roughly complementary properties were selected for inclusion in the system (see Table 1). Only three of the four spectrometers are present at any one time: the ^{3}He Ionisation Chamber, one of the two Liquid Scintillator detectors (the choice depending on the yields expected from JET), and the Proton Recoil Telescope. The spectrometers are detailed in Sections 3.2 - 3.4 below, and their disposition within the shield is discussed in Section 3.5.

The adjustable aperture cannot, of course, be optimised for all the spectrometers simultaneously. The best setting depends not only on the expected yield, but also on which spectrometer would provide the most valuable information. This is discussed in Section 3.6.

3.2 ^{3}He Gridded Ionisation Chamber

^{3}He spectrometers are based on the reaction

$$^3\mathrm{He} + \mathrm{n} -> \mathrm{p} + \mathrm{T},\ Q = 764\ \mathrm{keV}$$

and the energy of the neutron is measured via the ionisation which the charged reaction products generate as they slow down in the gas.

The particular device used in the present system is a commercially available unit, model FNS-1, manufactured by Jordan Valley Applied Radiation Ltd (Migdal Haemek, P.O. Box 103, Israel 10550). It consists of a cylindrical chamber 5 cm in diameter and about 36 cm long, filled to a pressure of ten atmospheres with a mixture of ^{3}He, methane and argon (see Fig. 4). The anode runs along the axis of the chamber, and is surrounded by a grid attached to guard rings. The function of the methane is to reduce the charge collection times, and the grid makes the height of the pulses from the chamber independent of the position of the reaction (apart from wall and end effects). The guard rings reduce gas multiplication at the ends of the anode, and define the sensitive volume to be 15 cm long. A calcium purifier for the removal of tritium is attached at one end of the chamber, and a shield made of a 2 mm layer of boron nitride sandwiched between two 1 mm layers of cadmium reduces the sensitivity of the device to slow neutrons. The operating voltage for the chamber is 3000 V.

As with all the spectrometers, as few electronic units as possible are placed in the cavity (for reasons of accessibility), and the rest are in a cubicle in the JET Diagnostics Hall. In the case of the ^{3}He chamber, the only units in the cavity are the pre-amplifier (which is supplied by the manufacturer of the chamber as an integral part of it) and is associated power supply. The signals from the pre-amplifier are sent via a 130 metre cable to the main amplifier (an Ortec model 673) in the Diagnostics Hall, and the output from that is shaped and sent to an ADC. A precision pulser sends test pulses to the pre-amplifier, and these appear in the spectrum as a narrow peak just above the true pulse height distribution. This peak provides a constant check on the gain and resolution of the electronics, and alterations in its shape during periods of high counting rate indicate the extent of pulse pile-up. All signal and HT cables between the Torus Hall and the Diagnostic Hall are of the 'superscreened' type [10], which has a high degree of immunity to electromagnetic interference. The cable in use at JET has a characteristic impedance of 75 Ω and is also anti-microphonic.

Prior to the installation of the spectrometer at JET, its response to monoenergetic neutrons was measured at several energies using neutrons from the T(p, n)^{3}He reaction, the protons being provided by the Harwell 5 MV Van de Graaff. These measurements are described by Loughlin et al. [11], and are only summarised here. (See alo ref. [12]). A typical pulse height spectrum is shown in Fig. 5. The peak marked 'a' is due to complete charge collection from the recoiling proton and triton. The plateau 'b' is due to incomplete collection, caused by an ion track striking a wall of the chamber, or beginning or ending outside the sensitive region. The recoil edges 'c' and 'd' are due to elastically scattered protons (from the methane) and ^{3}He ions respectively, while the large peak 'e' is produced by the unavoidable background of slow neutrons which have a very large reaction cross section with ^{3}He. Counts below the thermal peak are due to gamma rays. Only the full energy peak 'a' and part of the wall effect plateau 'b' can be used in the spectral analysis of the data, so for every useful count there are many which must be discarded (typically about fifteen, for a threshold 600 keV below the thermal peak).

The width of the full energy peak is only about 40 keV. However, the long wall effect plateau has an important effect on the unfolding of neutron spectra from the raw data, and the effective resolution (in the sense discussed

in Section 6.1.1) is actually about 70 keV. This is still narrow compared with resolutions typically offered by neutron spectrometers of comparable size.

There are two main limitations with this type of spectrometer. Firstly, an upper energy limit is imposed by wall effects, which begin to affect the response significantly when the range of the recoiling protons becomes comparable with the dimensions of the chamber. For the present system, this upper limit is approximately 3 MeV. Secondly, the relatively long charge collection times limit the maximum counting rate. In the present system, the collection times of up to 12 μs cause unacceptable pulse pile-up at total counting rates above about 5 kHz.

3.3 Organic Liquid Scintillators

The second spectrometer employed in the present system is a scintillator/photomultiplier combination. Two such devices are available for use, and the choice of which to install in the spectrometer cavity depends on the neutron yields expected from JET during the next operating period. Both use the organic liquid scintillator NE213. One has a scintillator cell 5 cm in diameter by 1 cm thick, and the other a cell 1 cm diameter by 1 cm thick. Their efficiency remains adequate at neutron energies as high as 6 - 8 MeV, and their maximum useful counting rate exceeds 100 kHz (although the latter advantage is offset to some extent by the shape of the reponse function, as described at the end of this section). Both of the devices were supplied by NE Technology of Sighthill, Edinburgh EH11 4BY, Scotland, UK.

The two detectors are nearly identical apart from the size of the cell, so the description below applies equally to both. A diagram of the larger device appears in Fig. 6.

The scintillator cell is a bubble-free type known as BA1. It is cylindrical with matt white interior walls, and it has a glass window in one of the circular faces. The curved wall accommodates a coiled tubular expansion chamber, which allows for thermal expansion of the liquid scintillator up to about 30°C. Incorporated into the glass window is a ^{22}Na gamma source and a Light Emitting Diode (LED). The ^{22}Na source emits gamma rays of 511 and 1275 keV, and is used to check the energy calibration of the system. The LED was originally intended to provide a second gain check, or even to be part of an

automatic gain control system, but its light output was found to be too variable for the present application, and it is not now used. The photomultiplier is a 10-stage fast linear focussed tube (EMI 9815B).

The photomultiplier is of course susceptible to magnetic fields, so the entire spectrometer is surrounded by a triple magnetic shield. This shield is identical to those used in the JET Neutron Emission Profile Monitor [13]. It consists of an inner cylinder of mu-metal 1 mm thick (closed at one end), an intermediate cylinder of radio metal 2 mm thick (also closed at one end), and an outer cylinder of mild steel 3 mm thick (closed at both ends, apart from a small hole for the cables). The three cylinders are electrically isolated from each other. This shielding is designed to provide protection up to about 0.15 T, and effective protection to at least 0.06 T has been demonstrated in the JET Neutron Emission Profile Monitor [14]. The fields recorded by the magnetic sensors in the spectrometer cavity are much less than this (< 1 mT).

No electronics external to the detector are required inside the cavity; the anode signal is sent directly to the processing modules in the Diagnostics Hall via a superscreened cable. Since the scintillator is sensitive to gamma rays as well as to neutrons, a Pulse Shape Discrimination (PSD) system is used to distinguish between the two types of event. The principle of the module used (a Link System model 5020) is detailed elsewhere [15, 16], but, briefly, it relies on the existence of both rapidly decaying and a slowly decaying component in the light from NE213, and the fact that neutrons and gamma rays excite the two in different proportions. A pulse fed to the 5020 is split internally and passed to two separate integrators, one of which integrates for a short time (ideally 0 to about 25 ns), and the other for a longer time (ideally 0 to about 400 ns*). At the end of the longer time, the ratio of the two integrals is taken. If this exceeds a preset value, the event is classed as a gamma ray; otherwise, it is classed as a neutron. Recognition of a neutron event causes a logic pulse to appear at the "neutron" output, and likewise a "gamma" pulse is produced for a gamma event. An analogue signal proportional to the total charge in the photomultiplier pulse (more strictly, to the result of the longer integration) is also available. This analogue signal, which is designed to be analysed by an ADC, can be produced for neutrons only, gammas only, or both. Other signals produced by the PSD unit include

* At JET, the long integration has been reduced to about 120ns to improve throughput, and the short integration has been increased to about 50ns because of the long superscreened cable between the detector and the PSD module.

"Live Time", which measures the time during which the unit is available for processing pulses.

The PSD units used in the present system have been modified by White [17] for use with 75 Ω cable and to allow the nature of the analogue signal to be changed (from neutron to gamma events, for example) under computer control during a JET discharge.

Fig. 7 shows the response of the larger spectrometer to monoenergetic neutrons (produced by the T(p, n)^{3}He reaction, as for the measurements on the ionisation chamber described earlier). The response follows basically the rectangular energy distribution of the recoiling protons, distorted by the non-linear light output function typical of protons (see, for example, ref. [18]) and smeared by the resolution of the system. This extended, largely featureless shape makes the unfolding of the original neutron spectrum from the measured data a difficult process, and is the main drawback of this type of spectrometer.

3.4 Proton Recoil Telescope

The third spectrometer employed in the present system is a proton recoil telescope. Incident neutrons scatter elastically from the protons in a thin plastic film (see Fig. 8(a)), and those protons which recoil in the forward direction are detected in a semiconductor detector. This limitation to forward directions only, imposed by the geometry of the device, results in a peaked pulse height distribution, which makes the extraction of the incident neutron spectrum a much easier task than for the liquid scintillator.

In the present device, the plastic film or 'proton radiator' is mounted on a thin stainless steel backing foil, and the assembly can be rotated 180° under remote control. In this reversed orientation (Fig. 8(b)), the stainless steel foil prevents protons from reaching the detector, allowing the background of unwanted events to be measured.

The design of this type of spectrometer is a compromise between efficiency and resolution. The efficiency can be increased by moving the detector closer to the proton radiator, or by using a larger radiator or detector, but this degrades the resolution because of the increase in the range of accepted

proton recoil angles. In addition, thickening the radiator increases the interaction probability, but also increases the variation in the slowing down of the protons as they travel to the surface.

The configuration adopted for the present device is shown in Fig. 9. The silicon diode is a totally depleted device 220 microns thick and 2500 mm^2 in area (detector type MSX25-225-PCB, supplied by Micron Semiconductors Ltd of 1 Royal Buildings, Marlborough Road, Churchill Industrial Estate, Lancing, Sussex BN15 8UN, UK). It is mounted 150 mm behind a polypropylene ($(CH_2)_n$) radiator 0.75 mg/cm^2 thick and 60 mm in diameter. A mixed nuclide alpha source (Amersham International type AMR 43) is mounted behind the detector, and provides calibration peaks at 5.157, 5.486 and 5.806 MeV. The backing foil for the proton radiator is 75 μm thick.

The range of 2.5 MeV protons in air at atmospheric pressure is only about 10 cm, so the whole spectrometer mechanism is mounted in a vacuum chamber and kept at a pressure of less than 0.08 mbar. The central regions of the windows of the chamber are thinned to 0.8 mm to reduce neutron scattering.

The efficiency and resolution of the spectrometer have been measured to be 1.22×10^{-4} per n/cm^2 and 230 keV (FWHM) respectively, using 2.5 MeV neutrons generated by the 500 kV Van de Graaff at Harwell. Fig. 10 shows a typical response function. Measurements of the effect of 14 MeV neutrons were also made, and indicated that at JET (where the ratio of 14 MeV flux to 2.5 MeV flux is about 1%) a low but measurable background under the peak was to be expected from this source. Fig. 11 shows two spectra measured at JET, one with the radiator assembly in the normal orientation and one with it rotated. The total background in the region of the proton peak is only about 15%.

The electronics for this device are as follows. The semiconductor detector within the vacuum chamber is connected to an external pre-amplifier by a short length of superscreened cable and a vacuum sealed coaxial feedthrough. The pre-amplifier (Canberra model 2004) is connected to a spectroscopy amplifier (Canberra 2021) in the Diagnostics Hall by a superscreened cable, and the output from this amplifier is fed to an ADC. The vacuum chamber and the pre-amplifier are surrounded by a copper

screen (connected to the earth of the electronics in the Diagnostic Hall) to protect the system against electrical interference from other JET devices such as stepper motors and turbomolecular pumps.

The high count-rate capacity of this device (up to about 100 kHz), coupled with its low efficiency, means that it is ideally suited for studies of the highest yield D-D régimes of JET.

3.5 Disposition of the Spectrometers Within the Enclosure

The arrangement of the spectrometers within the shield is shown in Fig. 3. The Proton Recoil Telescope has very little material in the beam, and therefore produces least scattering and spectrum distortion, so this spectrometer is placed at the front. The Liquid Scintillator, on the other hand, is surrounded by a heavy magnetic shield, which presents a substantial target to the beam; this device is therefore placed at the rear, downstream of the high resolution ^{3}He chamber.

3.6 Setting the Adjustable Aperture in the Collimation

The appropriate size of the adjustable aperture is estimated from the neutron yield expected from the next discharge, having regard to which of the spectrometers would produce the most valuable information. The latter decision is based on the following principles.

The ^{3}He ionisation chamber is the preferred device for general use, because of its high resolution. However, it has a count rate limit of about 5 kHz, and in addition only about one in fifteen of all counts falls in the useful region of the reponse. This means that at least 2½ seconds are necessary to accumulate enough counts for analysis, and at JET periods of high neutron output are frequently shorter than this. In such cases the aperture is optimised for one of the other spectrometers, and analysis of ^{3}He data is confined to periods of the discharge in which the counting rate happens to be satisfactory.

The scintillator is usually chosen for high power ICRH discharges (even if the ^{3}He chamber would be usable) because of its sensitivity to the high energy neutrons which ICRH can produce.

The Proton recoil telescope is usually used for very high yield discharges, or for cases where the additional heating is too brief for the ^{3}He chamber to be useful. The aperture is widened to its maximum for this instrument.

4. AUXILIARY SYSTEMS AND SENSORS

The environment within the shielded enclosure is maintained and monitored by the following auxiliary systems and sensors.

4.1 Chiller Unit

A refrigeration system keeps the temperature inside the spectrometer cavity at about 15°C. This system consists of an evaporator bolted to the roof of the cavity, connected by piping to a compressor on top of the shield. The system is automatically switched off during a JET discharge so that vibrations from the evaporator in the cavity do no interfere with the highly microphonic ^{3}He chamber.

4.2 Temperature Probes

Three probes monitor the temperature at selected points inside the cavity. These probes are of the RTD (Resistance Temperature Detector) type based on the resistance of a platinum element. RTDs were chosen in preference to thermocouples because of the lack of a suitable place for the cold junctions of the latter. Each probe is connected to a small transmitter unit inside the cavity which encodes the temperature measurement as a current level between 4 and 20 mA. Since the Liquid Scintillators can suffer from the formation of bubbles in the cell at high temperatures, one of the probes is always placed inside the photomultiplier's magnetic shield. A current-sensing relay is connected to the transmitter signal from this probe, and this switches the photomultiplier HT off automatically if the temperature rises above the safe limit (about 28°C).

4.3 Magnetic Field Sensors

During a discharge, the changing magnetic fields inside the cavity induce voltages in three mutually perpendicular search coils. Integrating these voltages (using electronics of JET design) gives the field strength as a

function of time. The calibration of the system was based on data supplied by JET [19].

4.4 Microphone

Since the ^{3}He chamber in particular is sensitive to sound, a microphone is included so that the noise levels in the cavity can be monitored if required.

5. MONITORING AND DATA ACQUISITION

5.1 Monitoring of the Status of the Instruments

The status of the instruments (the HT setting, the vacuum pressure, the leakage current, etc.) is monitored using the JET MIMIC system [9]. This allows the values of parameters of interest to be displayed on a VDU, together with a schematic diagram of the instrument or system. Fault conditions can be highlighted in a suitable colour.

5.2 Data Acquisition

The data acquisition is controlled by the JET "CODAS" system [9]. Immediately prior to a discharge, the recording electronics for each instrument are programmed with a predetermined set of instructions, and then a trigger signal is issued at the appropriate moment. The acquisition of the data is essentially independent of the central CODAS computers. At the end of the discharge, the recording units are interrogated and their data incorporated into the JET Pulse File for that discharge.

The principal recording electronics for the ^{3}He spectrometer consists of an ADC (LeCroy model 3512) connected to a 64K memory module. During a discharge, pulses from the main amplifier are analysed into 256 pulse height bins in a segment of this memory. Every 0.5 seconds, the segment number is incremented, allowing the spectrum to be recorded as a function of time. Another module - a latching scaler - records the triggering rate of the main amplifier as a function of time by counting the number of pulses from the amplifier's Count Rate Monitor over periods of 12 ms throughout the discharge.

For the NE213 scintillators, the analogue data are recorded in much the same way. The chief difference is that in the 20 seconds prior to plasma formation, and the 15 seconds after decay, the analogue output of the PSD unit is automatically switched from neutron pulses to gamma pulses, allowing a spectrum from the built in ^{22}Na calibration source to be collected. The rates of neutron and gamma events throughout the discharge are recorded as a function of time by latching scalers. In addition, the PSD unit's "Live Time" signal, which is a logic level rather than a pulse, is recorded by using it to gate a 100 kHz oscillator. The interrupted pulse train is fed to a latching scaler, and subsequently analysis yields the percentage Live Time as a function of time.

Analogue data from the main amplifier of the Proton Recoil Telescope are recorded as for the ^{3}He chamber.

Data from the auxiliary sensors are also recorded and incorporated into the JET Pulse File. The integrators attached to the magnetic field probes produce a varying voltage proportional to the field strength; this is sampled at 12 ms intervals by a Transient Analysing ADC. Slower or static signals (such as the Voltage Monitor signal from the HT unit on the ^{3}He chamber, or the servo signals from the adjustable aperture) are sampled once per discharge by a Single Shot ADC. The values of the HTs applied to the photomultipliers are obtained by interrogating the LeCroy HV4032A HT unit.

6. ANALYSIS

Most of the analysis of the data from the system is done using the general purpose neutron analysis package SNAP. This package allows a wide variety of display and analysis operations to be carried out on spectra and other data from many different JET diagnostic instruments. The chief analysis techniques used on spectra from the system described here are as follows.

6.1 Data from the ^{3}He Ionisation Chamber

The calibrations at Harwell, described in Section 3.2, of the ^{3}He chamber allowed its response to monoenergetic neutrons to be parameterised as a function of neutron energy between 2.0 and 3.0 MeV. Referring again to the typical monoenergetic response shown in Fig. 5, the parameterisation chosen

to describe the response at a given neutron energy, from the full energy peak to part way along the wall effect plateau, was as follows. The full energy peak was fitted by a sum of two Gaussians, requiring five adjustable parameters (the width and position of the upper Gaussian, the width of the lower, their separation, and the ratio of their heights). A sixth parameter was used to describe the wall effect, and a seventh specified the overall normalisation. This is described in detail by Loughlin et al. [11]. Some of the parameters were found to vary linearly with neutron energy, and the others remained constant.

This parameterisation is used to derive the JET neutron spectrum from the measured data by a 'forward calculation'. An initial estimated spectrum shape is folded with the response function to produce a model pulse height distribution, and this is compared with the real data. The spectrum shape is refined iteratively to minimise the discrepancy (as measured by chi-squared) between the model and real distributions. The details of this process depend on the type of JET discharge being analysed, as described in Sections 6.1.1 - 6.1.3.

6.1.1 ^{3}He Data Analysis for Ohmic Discharges

For ohmic discharges, the neutron spectrum can be assumed to be Gaussian in shape. The fitting procedure outlined above is used to find the centroid and width of this Gaussian, and the plasma temperature can be found from the width in the manner described in Section 1.4. An example of unfolding with this method is given in Fig. 12.

An "effective resolution" for the spectrometer can be found by subtracting in quadrature the width of the unfolded spectrum from the width of the full energy peak in the raw data (the latter width being measured by fitting with a Gaussian on a complementary error function). The result for JET data is typically about 70 keV, which is substantially greater than the 40 keV width of the full energy peak in the monoenergetic response (see Section 3.2). This difference is understood to be due to the wall effect plateau (feature 'b' in Fig. 5), which, although low, adds a long tail to the response function (see the discussion in ref. [20]).

6.1.2 ^3He Data Analysis for Additionally Heated Discharges

For plasmas heated by ICRH, the assumption of a Gaussian neutron spectrum can no longer be made with confidence, and for Neutral Beam heating the spectrum differs markedly from Gaussian. To analyse such discharges, the initial estimate of the spectrum is made in the form of a histogram, and the parameters which are optimised by the fitting procedure are simply the contents of the histogram bins. The number of bins is typically 7 to 11, and no constraints are applied on the shape of the histogram. Fig. 13 shows a typical histogram unfolded from an additionally heated discharge.

6.1.3 ^3He Data Analysis for Neutral Beam Heated Discharges

The neutron yield from discharges heated by neutral beam injection consists of contributions from reactions between fast beam ions and thermal ions (the 'beam-thermal' contribution), between thermal ions alone (thermal-thermal contribution), or between fast ions alone (beam-beam). For such discharges, a third analysis technique, in conjunction with theoretical models of fast ion behaviour, can determine the relative strengths of these contributions. Given the angle of beam injection and the angle at which the neutrons are observed, a program such as FPS [21, 6] computes theoretical shapes for the beam-thermal and beam-beam spectra. These are added to a Gaussian thermal-thermal spectrum, in estimated proportions, and the sum is used as an initial spectrum shape. The folding and fitting procedure described above then gives the best values of the relative proportions of each contribution, and (optionally) the temperature of the thermal component.

Analysis of this type is dicussed in detail by Loughlin et al. [22]. In this paper, the authors discuss how satisfactory fits to the data could only be obtained if the calculations included a population of ions streaming counter to the direction of injection. Such a population can arise when injected ions enter trapped orbits, in which they oscillate toroidally (magnetic mirror trapping). These trapped ions can only affect spectra obtained with a line of sight having a tangential component, and would not be evident from spectrometers which view the plasma radially.

6.2 Data from the NE213 Scintillators

A useful technique with these detectors is to compare the normalised count integral above a fixed threshold for discharges of different types. For example, Fig. 14 shows how high power ICRH heating can generate a population of high energy neutrons. This occurs when protons or deuterons are accelerated by the applied RF to high (possibly MeV) energies, and then interact with impurity ions to produce neutrons by a variety of nuclear reactions [23, 24]. In some discharges, the neutrons generated in this way can completely dominate the total yield, and without the information provided by the spectrometer, the measurements form other diagnostics (such as the yield monitors) could be misinterpreted.

Where unfolding of the spectrum is required, the code FLYSPEC [25] is used. This code is based on the differentiation of the recoil proton energy distribution. It requires the dependence of light output on proton energy to be specified, and the data used here are those due to Adams and Watkins [26]. These authors, noting the considerable discrepancies between NE213 light output functions in the literature (see, for example, refs. [27 - 29]), remeasured the light output from 1.5 to 3.2 MeV using a detector of the same type as those used here. The results were in excellent agreement with the function measured by Dekempeneer et al. [29].

6.3 Data from the Proton Recoil Telescope

The data taken at Harwell with D-D neutrons from the 500 kV Van de Graaff have been used to synthesise an energy-dependent response function by assuming that the shape of the response scales with neutron energy, and that the efficiency is proportional to the p(n, n)p cross section. The synthesised function is then used in SNAP to unfold spectra in the same way as described in Section 6.1.2 for ^{3}He data.

7. CONCLUSIONS. FUTURE EXPLOITATION

The spectrometry system described here is used routinely at JET for temperature measurements in suitable discharges. It is also particularly useful in studies of Neutral Beam heating (where its nominally tangential line of sight confers an

advantage) and in the interpretation of discharges where a substantial fraction of the neutron yield is of non-fusion origin.

The large shield has proved valuable for allowing the rapid installation of experimental detectors at JET. For sufficiently small devices, if offers a low-background location close to a horizontal port, with electrical services, refrigeration and environmental monitoring already provided. (For example, a new detector for 14 MeV neutrons, based on the principle of a proton recoil telescope with a thick radiator, has recently been deployed. This device is described in detail by Croft et al. [30]). It is expected that the future exploitation of the system will lie increasingly in this direction.

ACKNOWLEDGEMENTS

The authors would like to thank Drs S Croft and J M Adams for their helpful comments on the manuscript, and Dr G Sadler for valuable discussions and for his help in the preparation of the diagrams. Thanks are also due to Messrs J Reid and A Tiscornia for their help in installing the system, and to Dr D B Syme for his interest and encouragement throughout the project.

REFERENCES

[1] P H Rebut and B E Keen, Fusion Technology **11** (1) (1987) 13-42.

[2] O N Jarvis, G Gorini, M Hone, J Källne, G Sadler, V Merlo and P van Belle, Rev. Sci. Instrum. **57** (8) (1986) 1717-1722.

[3] T Elevant, D Aronsson, P van Belle, G Grosshög, M Hök, M Olsson and G Sadler, Nucl. Instrum. Meth. in Phys. Research **A306** (1991) 331-342.

[4] B E Keen (Editor), JET Joint Undertaking Progress Report 1990. EUR13493 EN, EUR-JET-PR8.

[5] H Brysk, Plasma Phys. **15** (1973) 611.

[6] P van Belle and G Sadler, "Basic and Advanced Diagnostic Techniques for Fusion Plasmas", Proc. of Course and Workshop, Varenna, Italy, September 3-13 1986. Vol 3, pp. 767-774. Eds. P E Stott, D K Akulina, G G Leotta, E

Sindoni and C Wharton. Publ. Monotypia Franchi Città di Castello (PG) Italy, and the Office for Official Publications of the European Communities, Luxembourg. EUR 10797 EN. ISBN 92-825-7436-9.

[7] O N Jarvis, G Gorini, J Källne, V Merlo, G Sadler and P van Belle, Nuclear Fusion **27** (11) (1987) 1755-1763.

[8] D W Glasgow, D E Velkley, J D Brandenberger, M T McEllistrem, H J Hennecke and D V Breitenbecher, Nucl. Instrum. Meth. **114** (1974) 521.

[9] H van der Beken, C H Best, K Fullard, R F Herzog, E M Jones and C A Steed, Fusion Technology **11** (1) (1987) 120-137.

[10] E P Fowler, United Kingdom Atomic Energy Authority Report AEEW - M1361 (1975).

[11] M J Loughlin, J M Adams and G Sadler, Nucl. Instrum. Meth. in Phys. Research **A294** (1990) 606-615.

[12] M J Loughlin, PhD Thesis (1988), University of Birmingham, UK.

[13] J M Adams (1991), to be published.

[14] J M Adams (1991), private communication.

[15] G White, Proc. 2nd Ispra Nuclear Electronics Symposium, Stresa, Italy, May 20-23 1975. Publ. Commission of the European Communities, EURATOM, Luxembourg. EUR5370e (June 1975) 447-451.

[16] J M Adams and G White, Nucl. Instrum. Meth. **156** (1978) 459-476.

[17] G White (1988), private communication.

[18] F D Brooks, Nucl. Instrum. Meth. **162** (1979) 477-505.

[19] H Altmann (1988), private communication.

[20[G Gorini, M Hone, O H Jarvis, J Källne, V Merlo, G Sadler and P van Belle, "Basic Physical Processes of Toroidal Fusion Plasmas", Proc. of Course and

Workshop, Villa Monastero, Varenna, Italy, August 26-September 3 1985. Vol. 1, pp. 133-140. Eds. G P Lampis, M Lontano, G G Leotta, A Malein and E Sindoni. Publ. Monotypia Fanchi Città di Castello (PG) Italy, and the Office for Official Publications of the European Communities, Luxembourg. EUR 10418 EN. ISBN 92-825-6629-3.

[21] G Sadler, P van Belle, M Hone, O N Jarvis, J Källne, G Martin and V Merlo, 13th European Conf. on Controlled Fusion and Plasma Heating, Schliersee, 14-18 April 1986. Europhysics Conference Abstracts vol. 10C part 1, eds. G Brifford and M Kaufmann, publ. European Physical Society.

[22] M J Loughlin, P van Belle, N P Hawkes, O N Jarvis, G Sadler and D B Syme, Nucl. Instrum. Meth. in Phys. Research **A281** (1989) 184-191.

[23] G Sadler, J M Adams, P van Belle, T Elevant and O N Jarvis, Bull. Am. Phys. Soc. **33** (9) (1988) 2030.

[24] G Sadler, O N Jarvis, P van Belle and J M Adams, 15th European Conf. on Controlled Fusion and Plasma Heating, Dubrovnik, May 16-20 1988. Europhysics Conference Abstracts vol. 12B part 1, eds. S Pesic, and J Jacquinot, publ. European Physical Society.

[25] D Slaughter and R Stout, Nucl. Instrum. Meth. **198** (1982) 349-355.

[26] J M Adams and N Watkins (1988), private communication.

[27] V V Verbinski, W R Burrus, T A Love, W Zobel, N W Hill, and R Textor, Nucl. Instrum. Meth. **65** (1968) 8-25.

[28] D L Smith, R G Polk, and T G Miller, Nucl. Instrum. Meth. **64** (1968) 157-166.

[29] E Dekempeneer, H Liskien, L Mewissen and F Poortmans, Nucl. Instrum. Meth. in Phys. Research **A256** (1987) 489-498.

[30] S Croft, D S Bond, and N P Hawkes (1992), to be published.

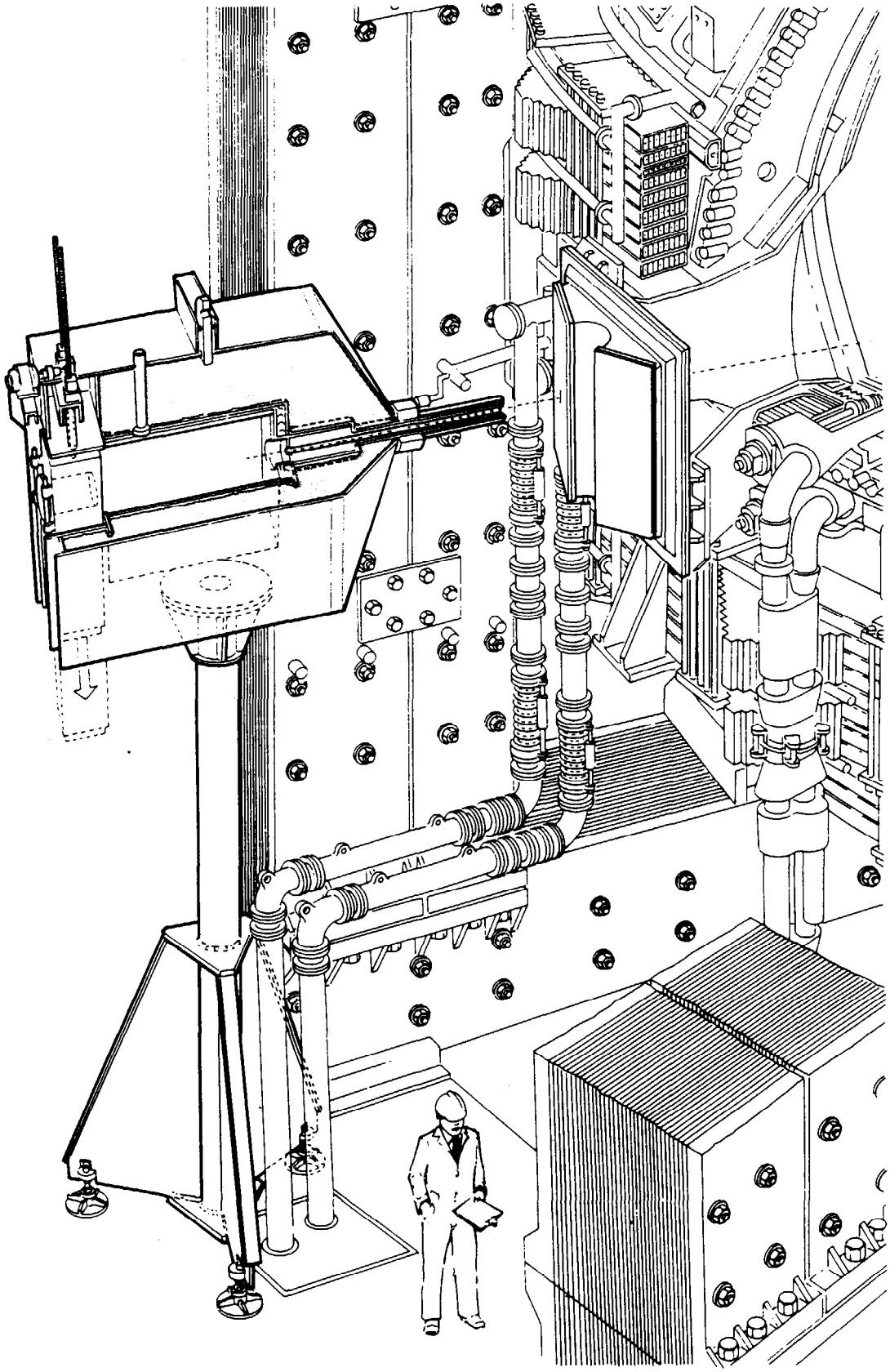

Fig.1 The shielded cavity and support tower. The adjustable aperture is not shown. Note that the shield and tower are now further from the JET machine than shown here.

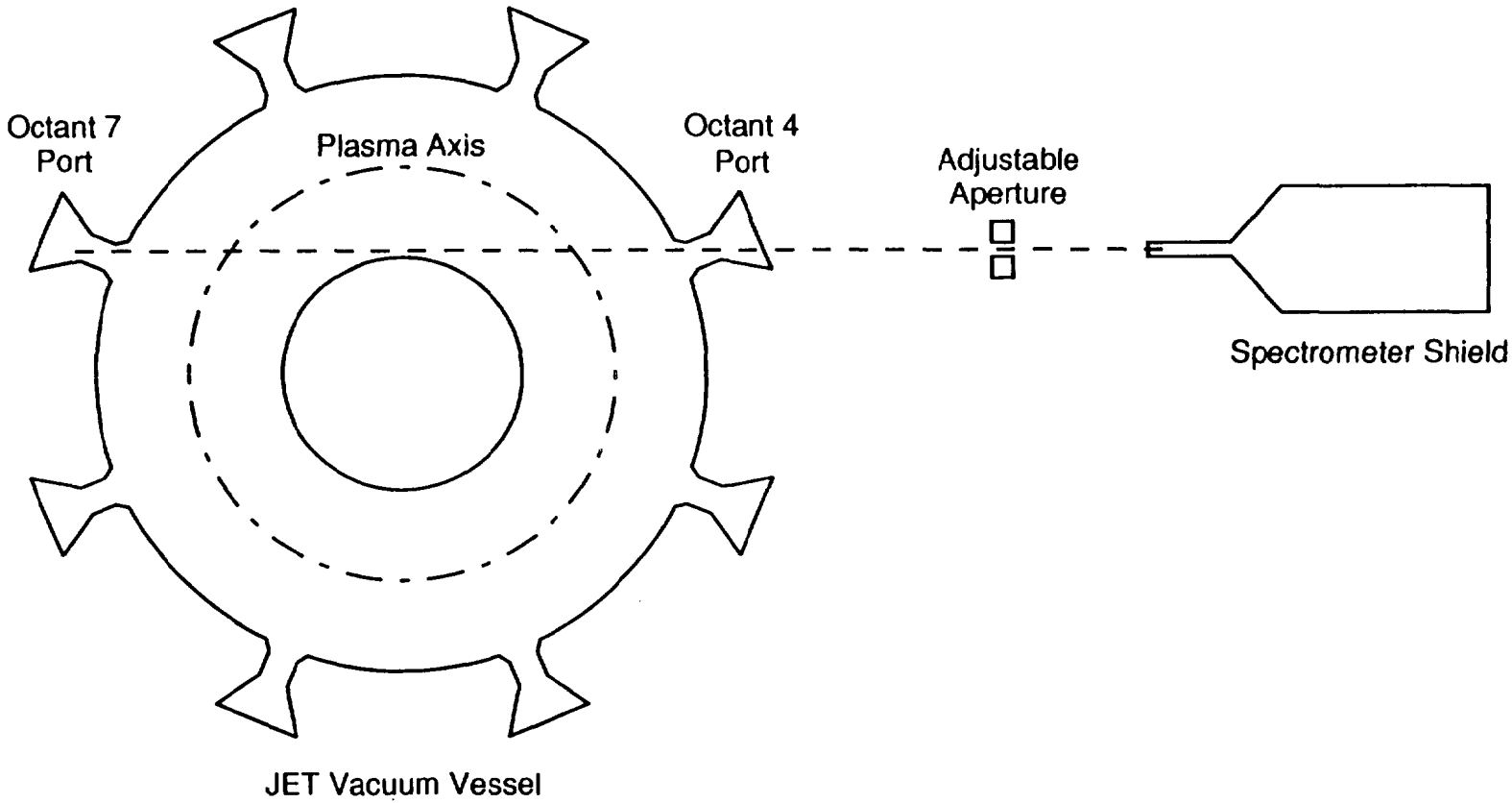

Fig.2 Line of sight for spectrometers.

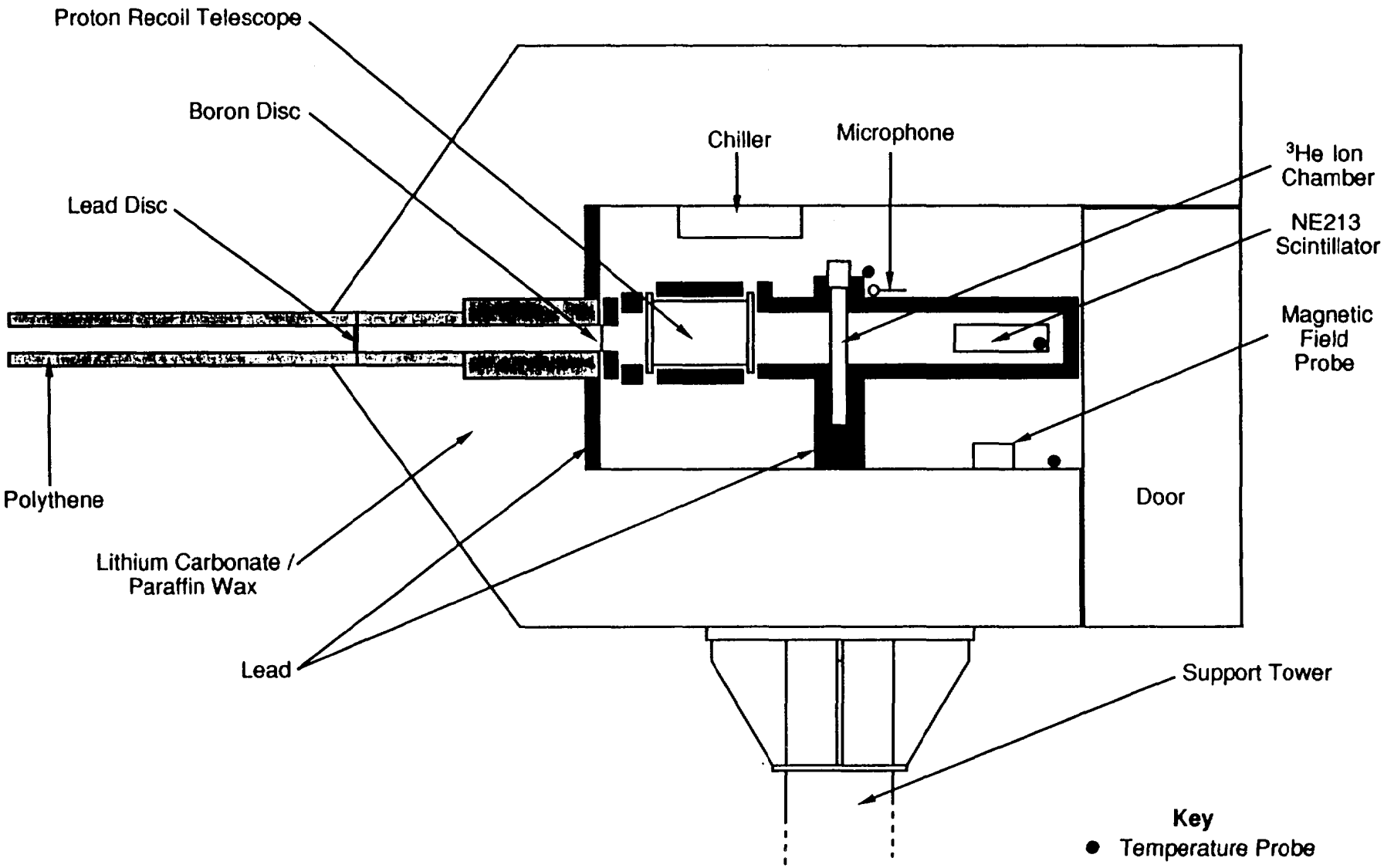

Fig.3 Interior of shielding block.

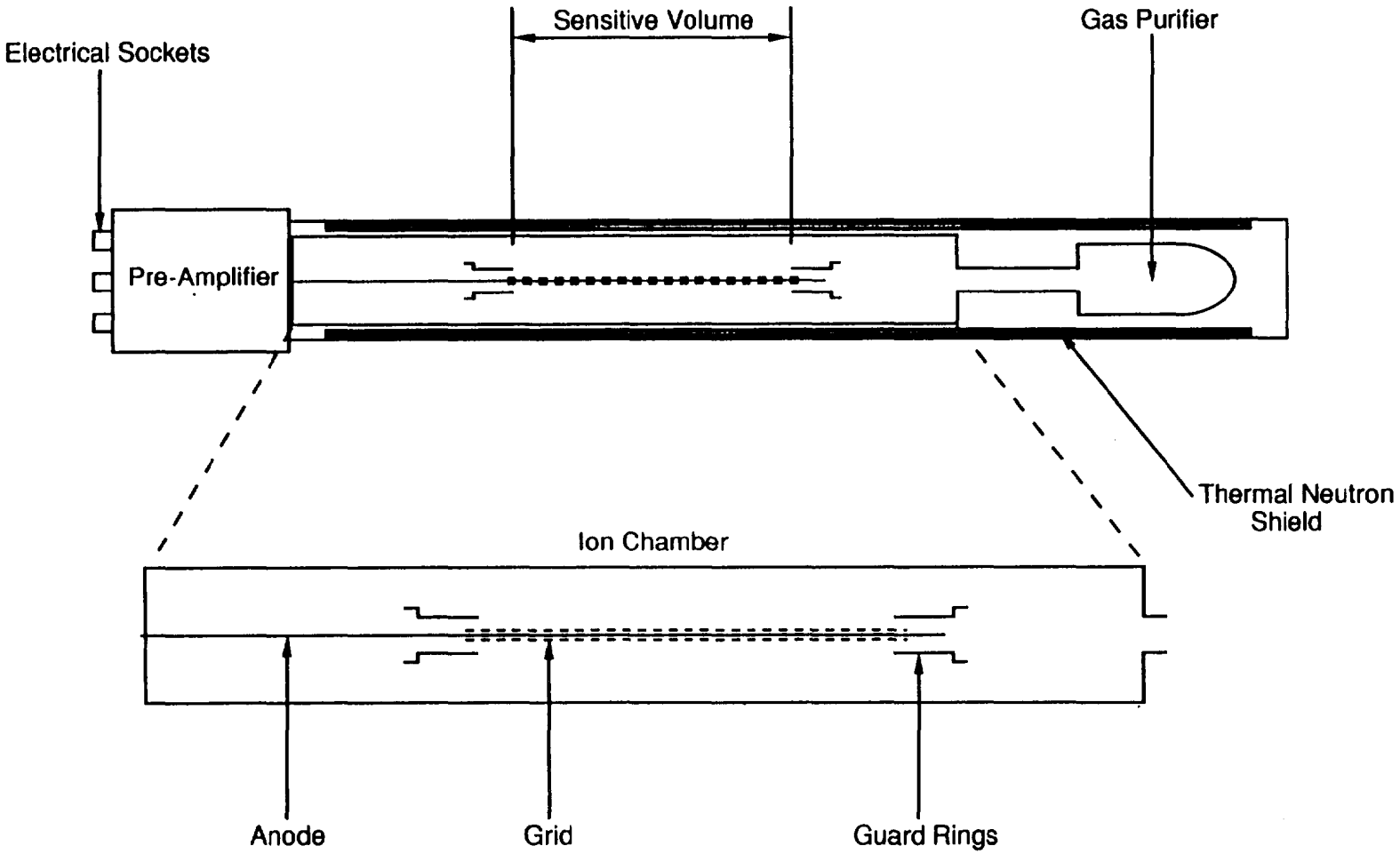

Fig.4 ^{3}He ionisation chamber.

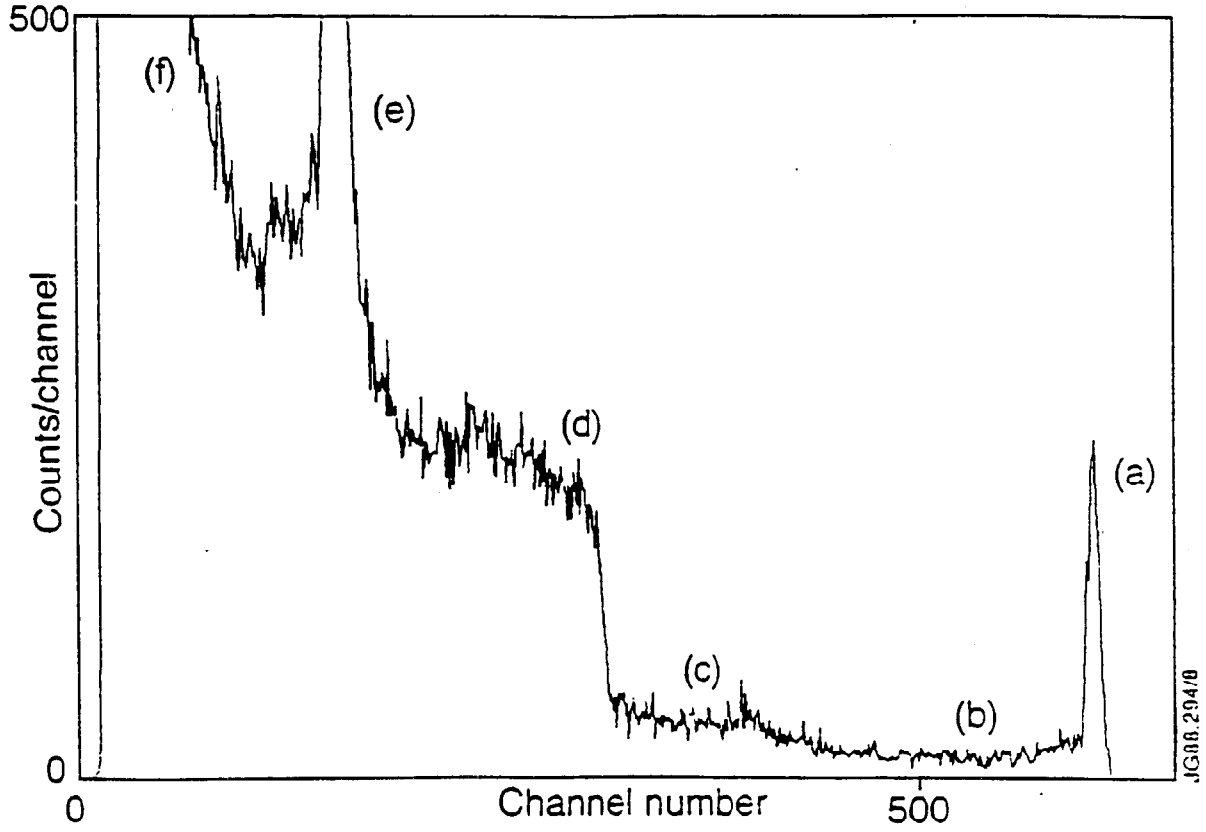

Fig.5 Response function of ^{3}He ionisation chamber to monoenergetic neutrons. (a) Full energy peak, (b) wall effect, (c) proton recoil events, (d) ^{3}He recoil events,, (e) the thermal peak, (f) low pulse height events due to gamma rays.

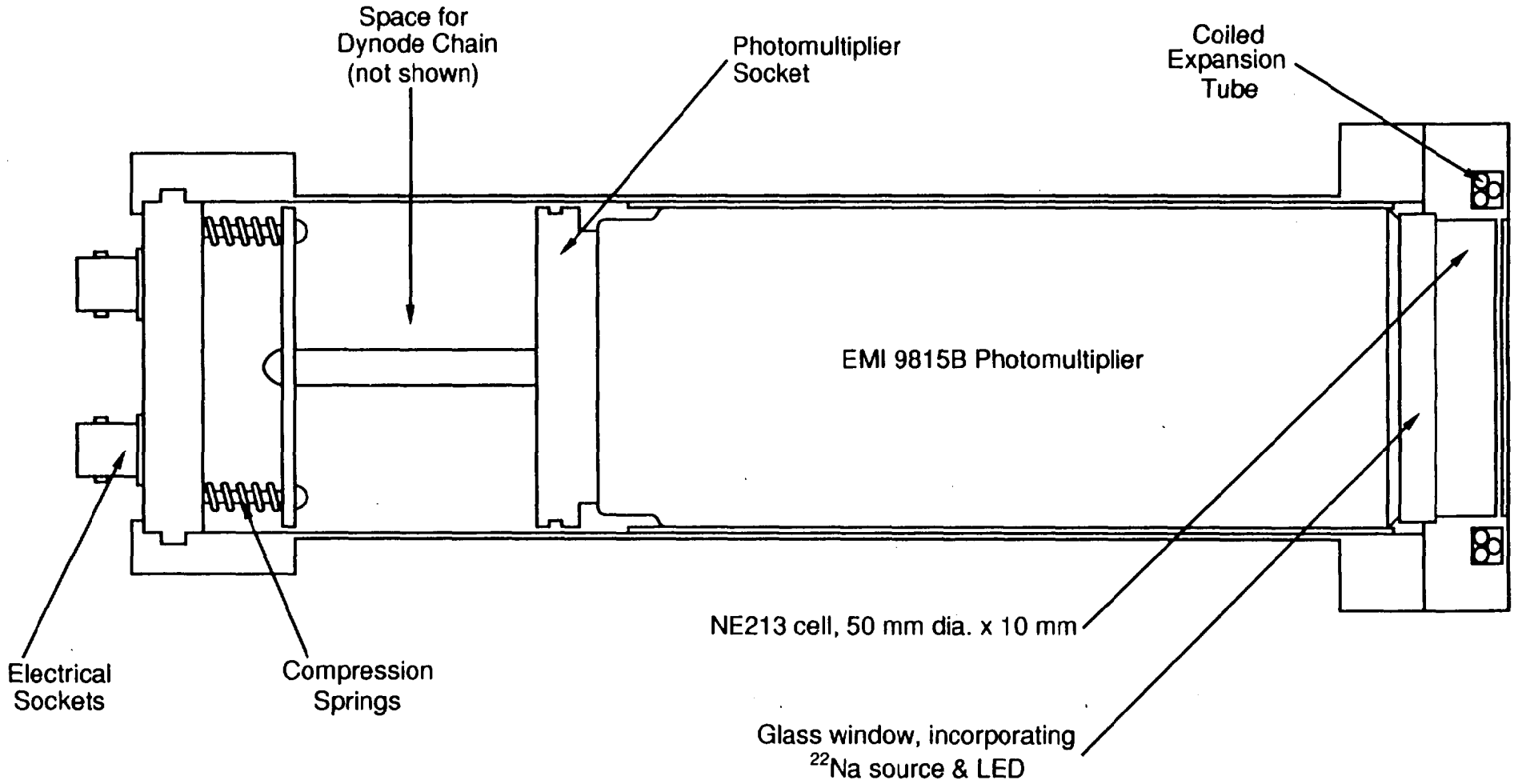

Fig.6 NE213 detector assembly.

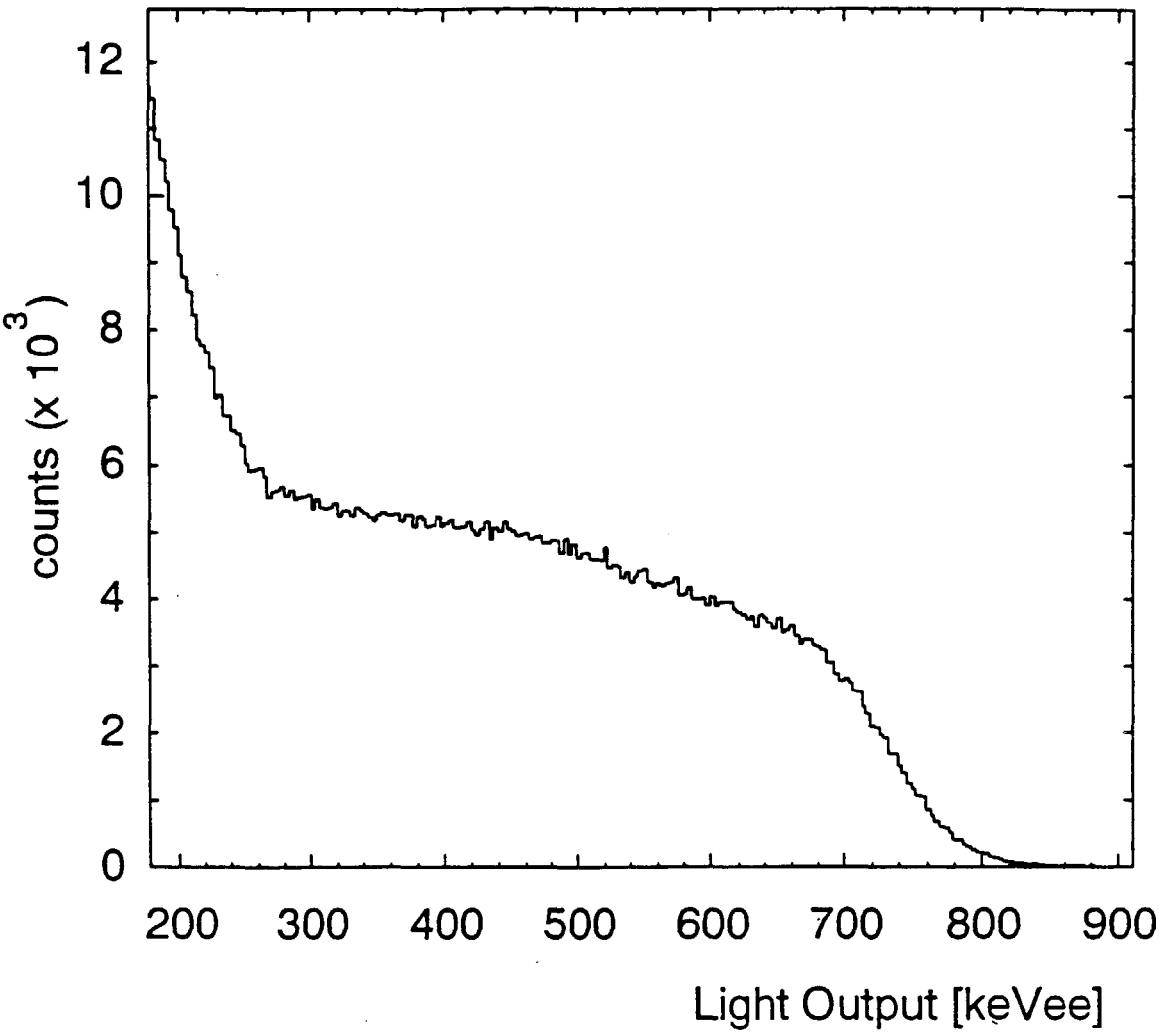

Fig.7 Reponse of large NE213 Scintillation Detector to monoenergetic neutrons of 2.56 MeV approximately. The light output axis is graduated in units of 'keV electron equivalent (ke Vee)', which are such that a 1 MeV electron stopping in the scintillator produces a light pulse of 1000 ke Vee.

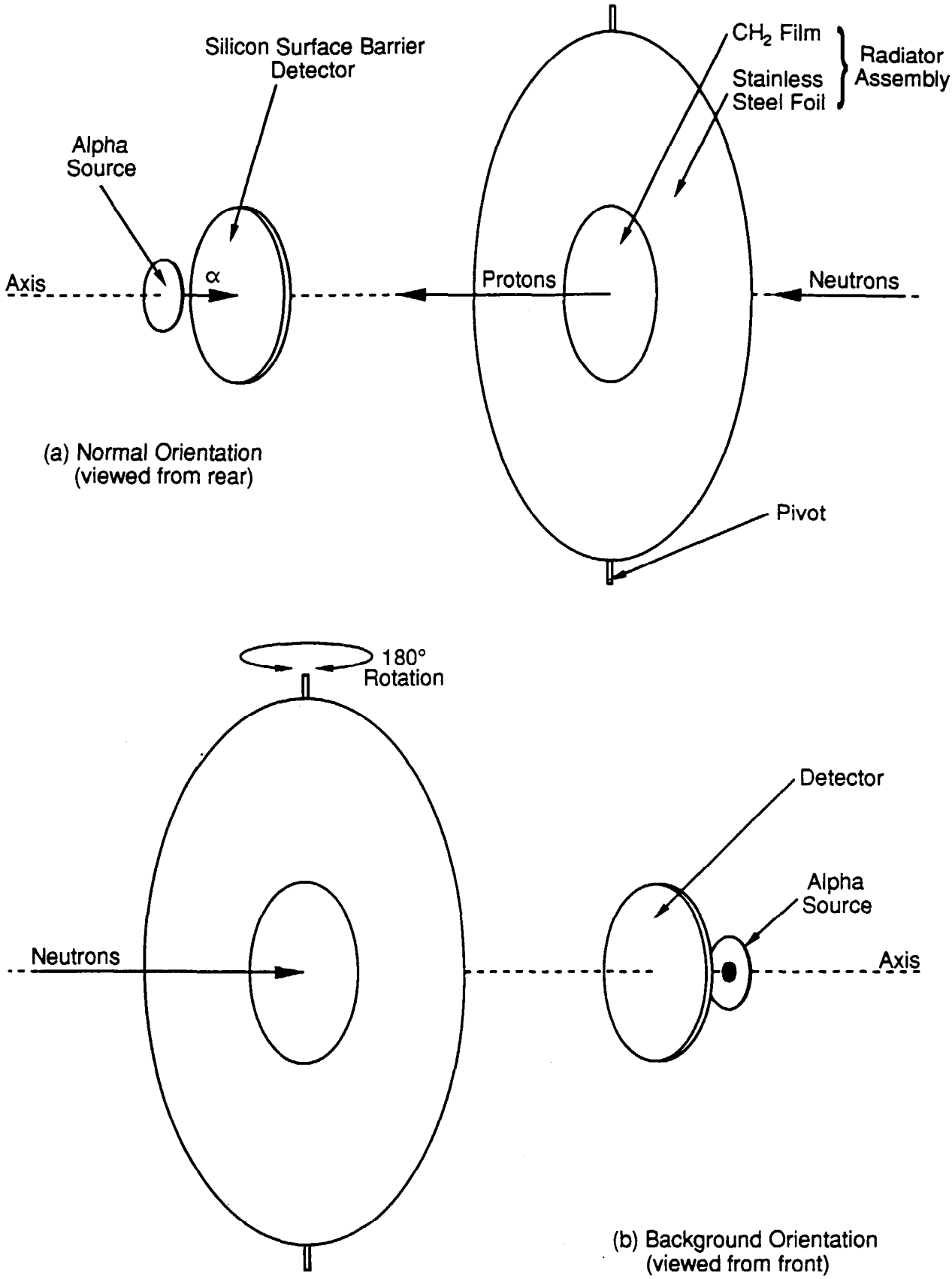

Fig.8 Principle of Proton Recoil Telescope.

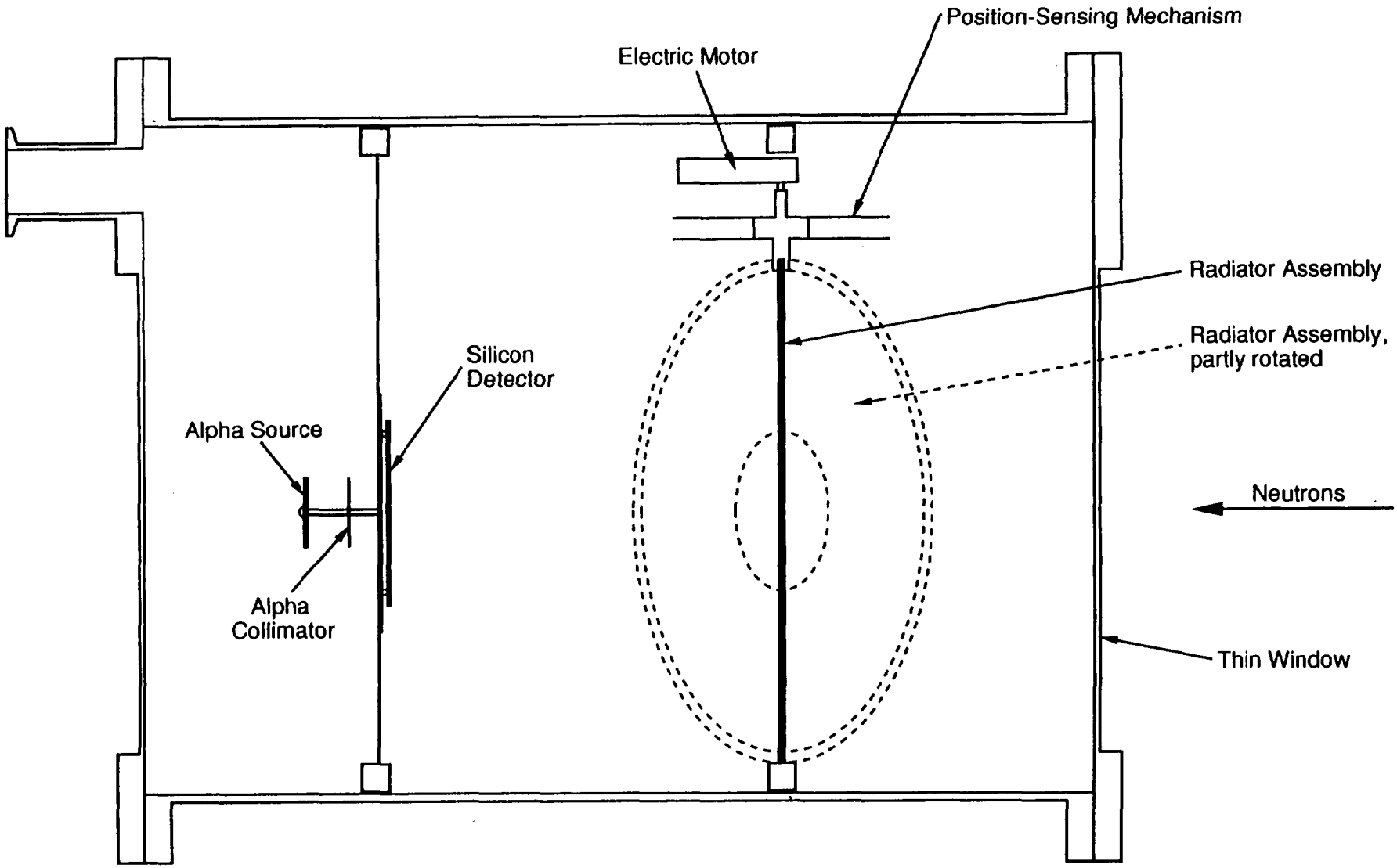

Fig.9 Proton Recoil Telescope.

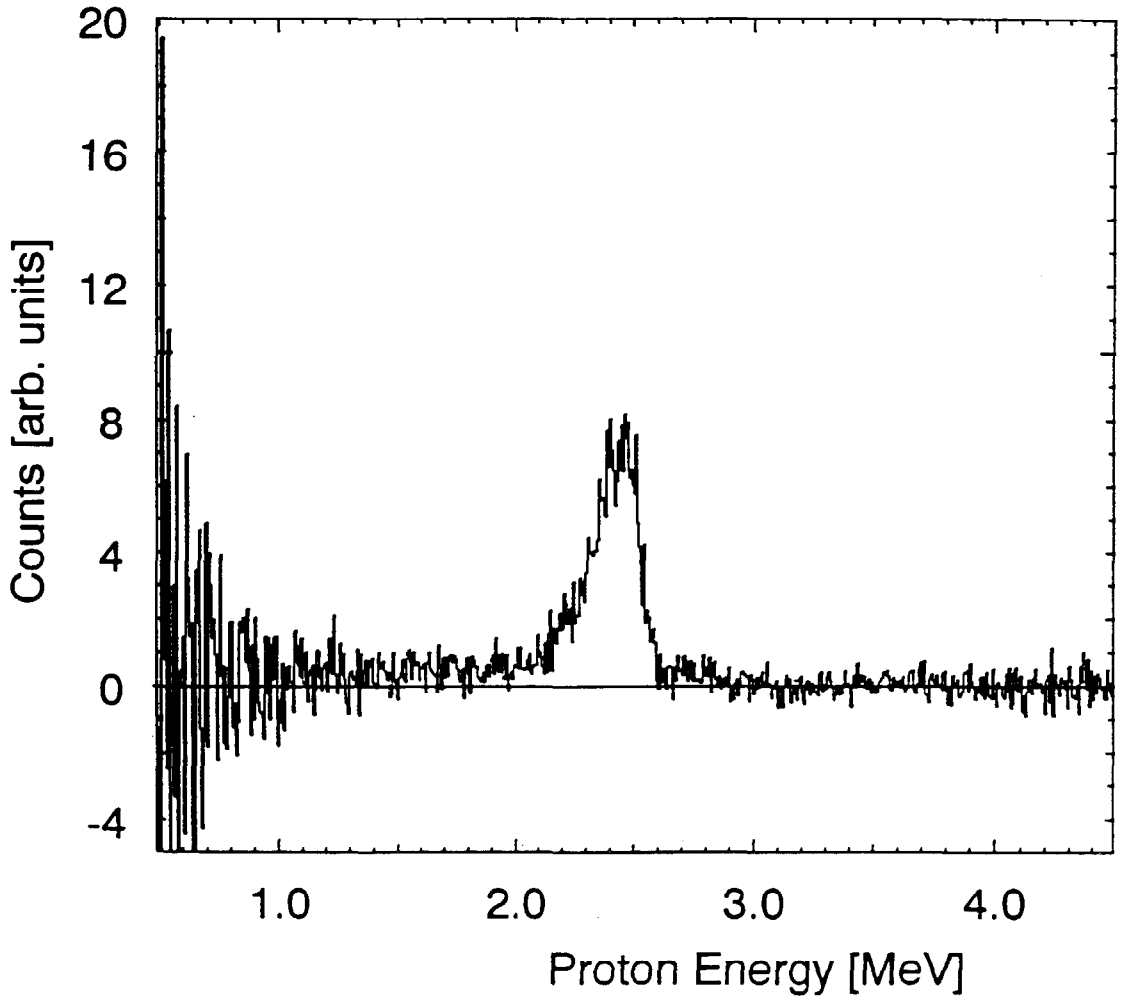

Fig.10 Response of Proton Recoil Telescope to monoenergetic neutrons (corrected for background).

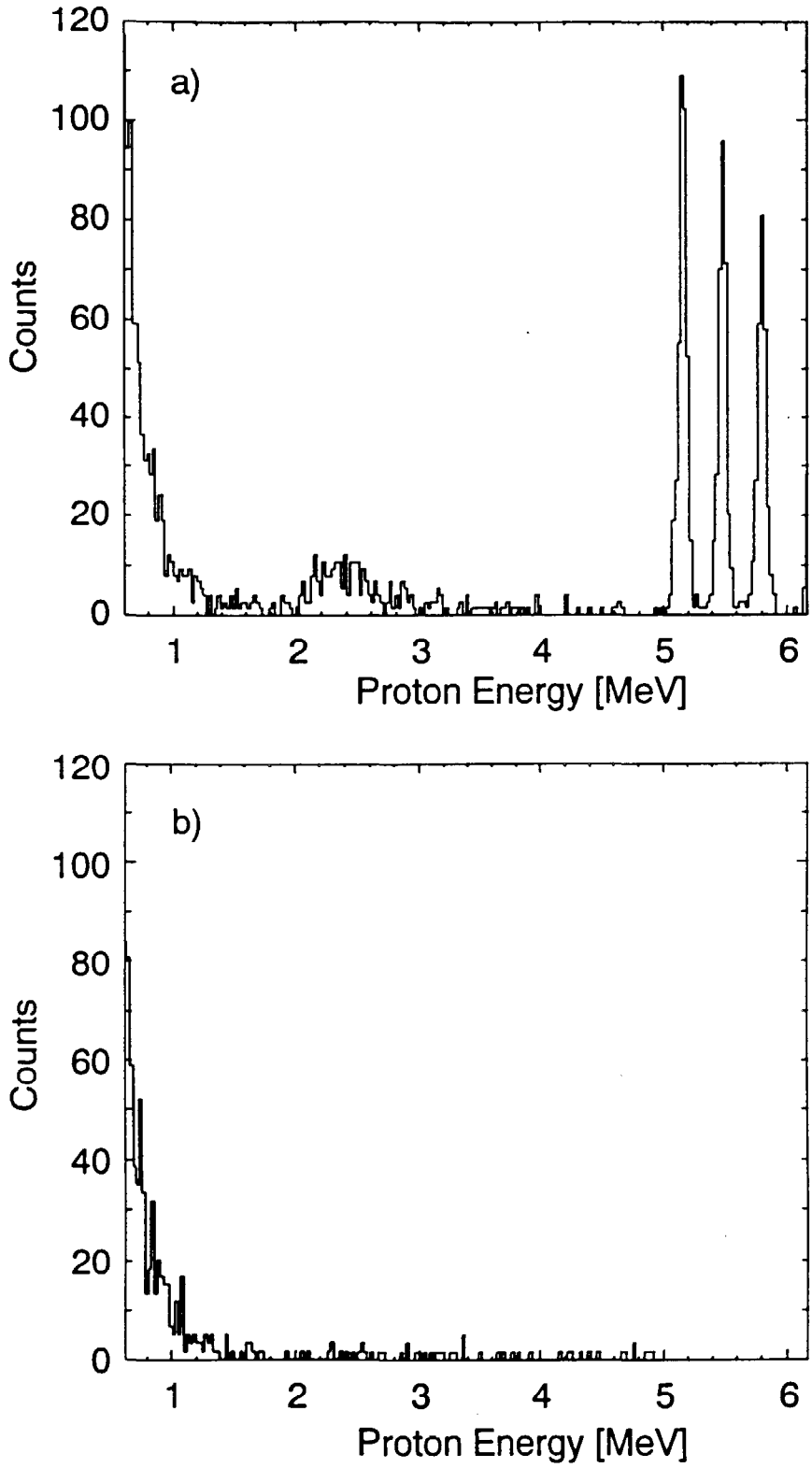

Fig.11 Two pulse height spectra taken at JET with the Proton Recoil Telescope. (a) Normal orientation of proton radiator assembly; (b) background orientation (see text). The spectra have been normalised to the same total neutron yield (10^{16}). The three sharp peaks on the right in (a) are from the mixed nuclide alpha source mounted behind the detector. The alpha peaks have been omitted from (b) for clarity.

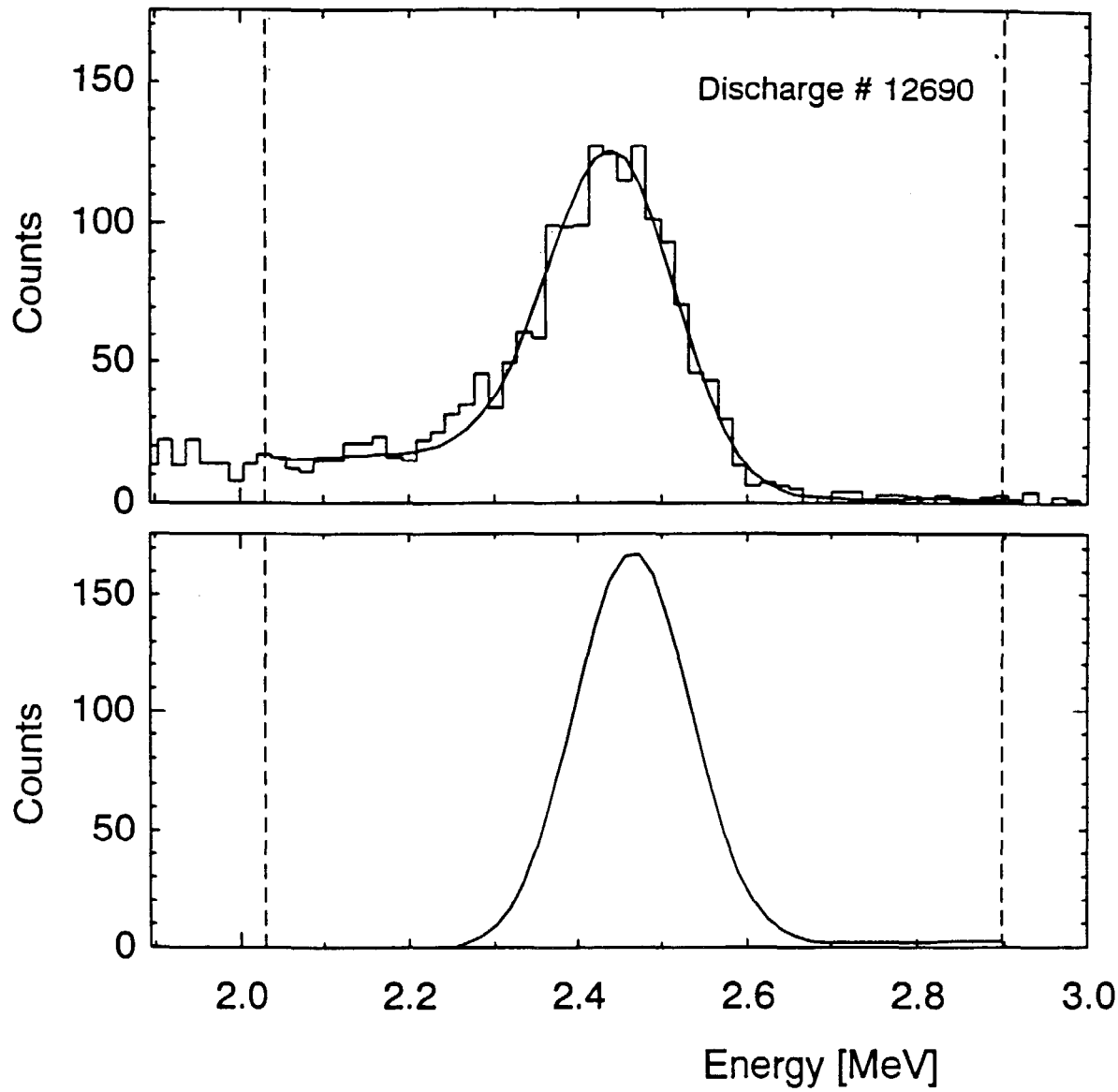

Fig.12 Unfolding a neutron spectrum from data from the ^{3}He chamber, for a purely ohmic discharge (in which the neutron spectrum is assumed to be Gaussian). Top: original data (histogram) and the convolution of the unfolded spectrum with the detector response (curve). Bottom: the unfolded Gaussian neutron spectrum.

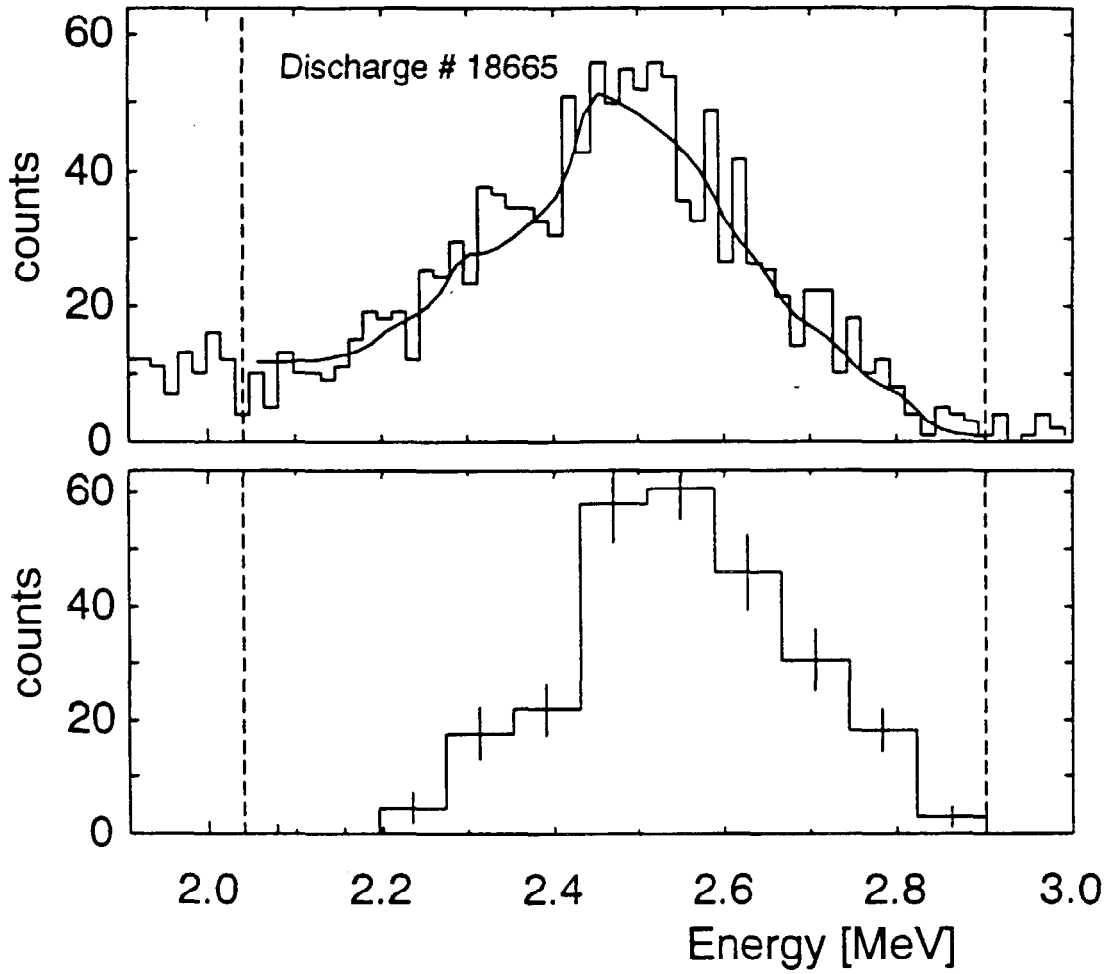

Fig.13 Unfolding a neutron spectrum from data from the ^{3}He chamber, for a discharge with NBI. Top: original data (histogram) and the convolution of the unfolded spectrum with the detector reponse (curve). Bottom: the unfolded spectrum. Note that the unfolded spectrum is markedly non-Gaussian.

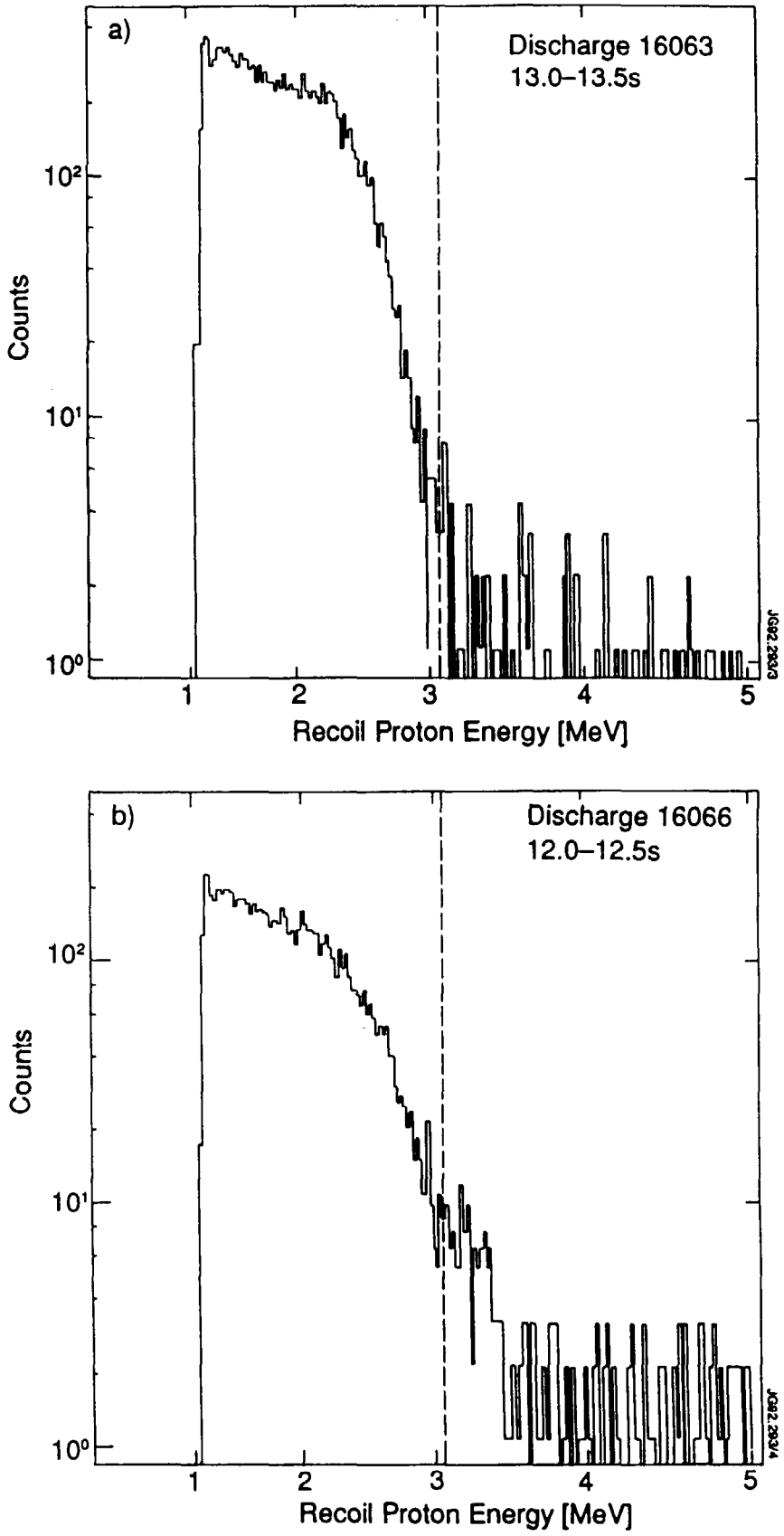

Fig.14 Pulse height spectra from one of the NE213 spectrometers. (a) A discharge without ICRH; (b) a discharge with high power ICRH. The presence of high energy counts is clearly visible in spectrum (b). These counts cannot be due to pulse pile-up, because the counting rate in (b) is very similar to that in (a).